THE JOURNAL OF PHYSICAL CHEMISTRY LETTERS
A JOURNAL OF THE AMERICAN CHEMICAL SOCIETY

pubs.acs.org/JPCL

Letter

Exploring the Blueprint of Photoprotection in Mycosporine-like Amino Acids

Abigail L. Whittock, Nazia Auckloo, Adam M. Cowden, Matthew A. P. Turner, Jack M. Woolley, Martin Wills, Christophe Corre, and Vasilios G. Stavros*

Cite This: *J. Phys. Chem. Lett.* 2021, 12, 3641−3646

Read Online

ACCESS | Metrics & More | Article Recommendations | Supporting Information

ABSTRACT: Microorganisms require protection against the potentially damaging effects of ultraviolet radiation exposure. Photoprotection is, in part, provided by mycosporine-like amino acids (MAAs). Previous reports have proposed that nonradiative decay mediates the impressive photoprotection abilities of MAAs. In this letter, we present the first ultrafast dynamics study of two MAAs, shinorine and porphyra-334. We demonstrate that, in aqueous solution, these MAAs relax along their S_1 coordinates toward the S_1/S_0 conical intersection within a few hundred femtoseconds after photoexcitation and then traverse the conical intersection and vibrationally cool in approximately 1 ps through heat transfer to the solvent. This new insight allows a quintessential component of microbial life to be unraveled and informs the development of molecular photon-to-heat converters for a myriad of applications.

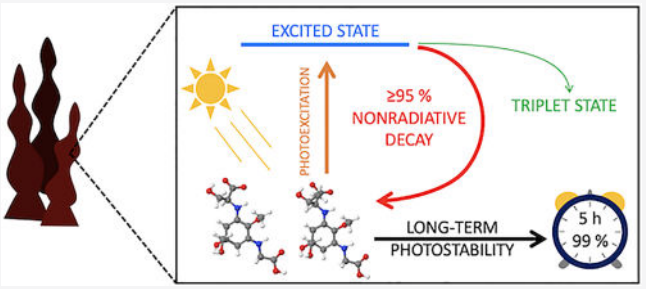

The harsh ultraviolet (UV) radiation on Archean Earth was one environmental stressor that nature was forced to respond and adapt to.[1] The evolution of natural UV protectants is uncertain; however, it has been suggested that mycosporine-like amino acids (MAAs) may be among some of the earliest UV-screening compounds.[1,2] MAAs remain key multifunctional molecules for microbial life and are biosynthesized by cyanobacteria, fungi, and algae.[3,4] While there are many proposed functions for MAAs, the focus of this present letter is to experimentally probe, at the molecular level, the origin of their photoprotective abilities.[4−9] MAAs are composed of either a cyclohexenone or cyclohexenimine core unit, while substituents on the ring result in variable peak absorptions in the UVA (400−315 nm) and UVB (315−280 nm), and molar extinction coefficients (ε) around 40 000 M^{-1} cm^{-1}.[3,5,10]

The two MAAs of interest presented here are shinorine and porphyra-334, shown in Figure 1. The photodecomposition, fluorescence, and triplet quantum yields for these MAAs have previously been reported.[11−13] Furthermore, photoacoustic calorimetry performed by Conde et al.[12] reported that MAAs release ∼97% of absorbed UV radiation as heat to their surroundings. While the above findings imply nonradiative decay to be the dominant relaxation mechanism, tracking this UV-to-heat energy transfer process in real time has remained elusive. Ultrafast spectroscopy can be used to track, and understand in unrivalled detail, energy flow; indeed, such studies have revealed energy transfer processes in MAA motifs[14−17] but not for the MAAs themselves. More broadly, an understanding of molecular photon-to-heat conversion

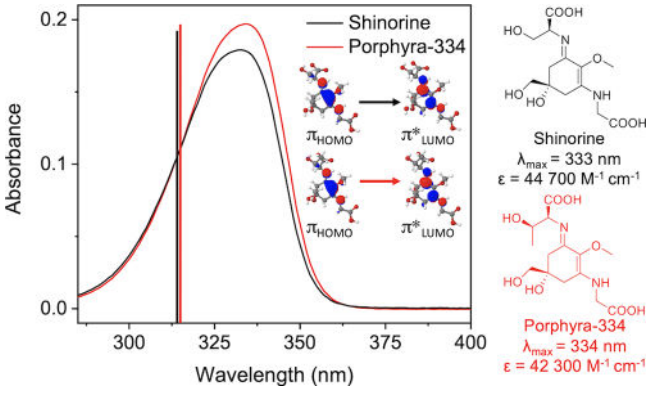

Figure 1. Experimental UV−visible spectra of 40 μM shinorine and 47 μM porphyra-334 in water. Theoretical predictions are presented as lines with the highest predicted oscillator strength normalized to the experimental absorption of porphyra-334. The corresponding orbitals are displayed as insets. Also shown are the structures of shinorine (black) and porphyra-334 (red), λ_{max} and molar extinction coefficient.[18,19]

Received: March 5, 2021
Accepted: April 5, 2021
Published: April 7, 2021

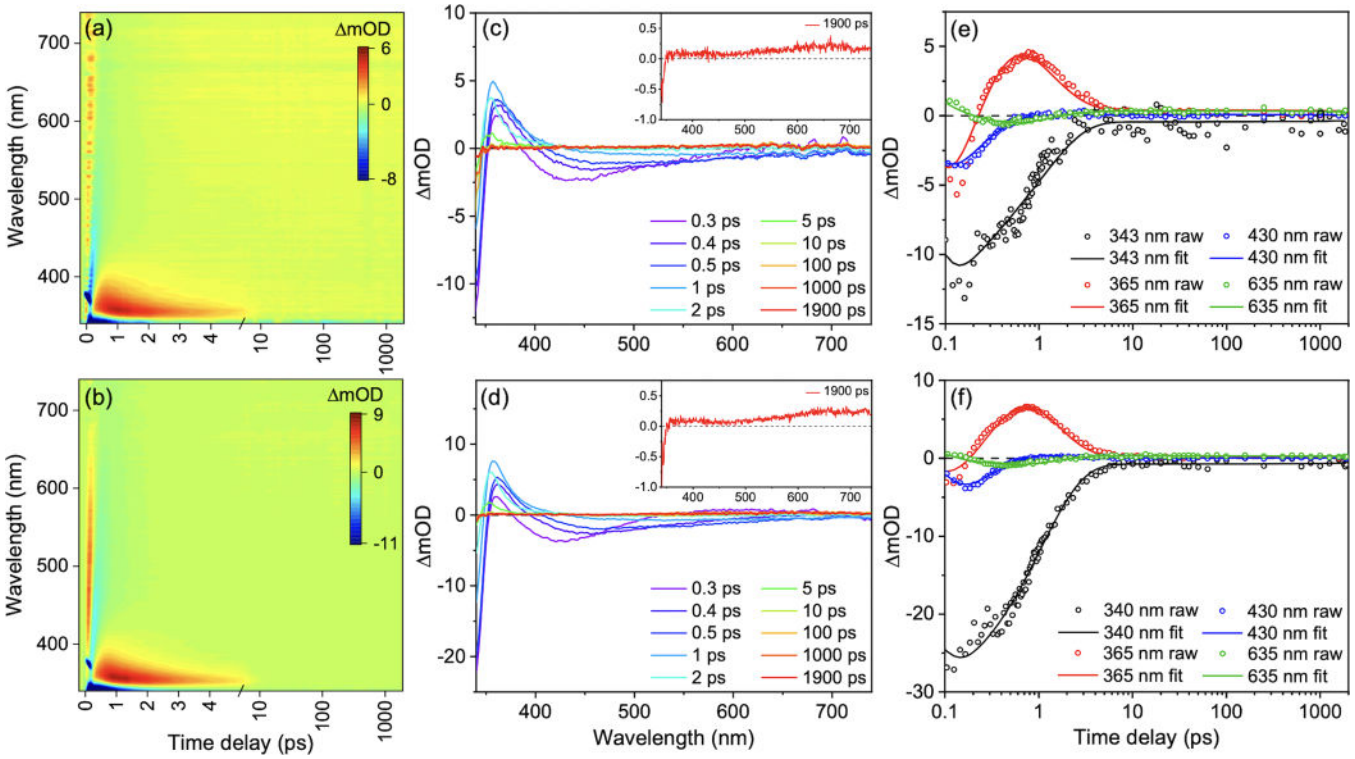

Figure 2. Transient absorption spectra (TAS) presented as false color heat maps for (a) shinorine and (b) porphyra-334 photoexcited at their respective λ_{max}. Time delays are plotted linearly until 5 ps and then as a logarithmic scale from 5 to 1900 ps. TAS presented as lineouts at selected time delays for (c) shinorine and (d) porphyra-334 photoexcited at their respective λ_{max}. The insets of (c) and (d) are TAS taken at 1900 ps. Transients at selected wavelengths for (e) shinorine and (f) porphyra-334 photoexcited at their respective λ_{max}. The open circles are the data, and the solid lines are the fit.

impacts environmental, medicinal, and cosmeceutical industries to name a few.

Here, we use transient electronic absorption spectroscopy (TEAS) to track the photoexcited state dynamics of shinorine and porphyra-334. Along with complementary theory and steady-state spectroscopic methods, we glean new insights into the photophysics of microbial life. Through probing, at the molecular level, how natural systems have evolved to withstand UV radiation, we can apply biological principles to the design of synthetic, biomimetic molecular photon-to-heat converters.

Shinorine and porphyra-334 were extracted and purified from Helioguard 365 (Mibelle Biochemistry),[20−23] a commercial product that contains extracts (from the red algae *Porphyra umbilicalis*) that consist of about 0.1% MAAs (dry weight). Experimental details can be found in section S1 in the Supporting Information. The UV−visible spectra of aqueous solutions of shinorine (λ_{max} = 333 nm) and porphyra-334 (λ_{max} = 334 nm) and their structures are given in Figure 1.

Using TURBOMOLE,[24] we calculated the vertical excitation energies of shinorine and porphyra-334 in their zwitterionic form, the form responsible for their strong UV absorption,[25,26] using the second-order approximate coupled-cluster singles and doubles method (RI-CC2) employed with the resolution-of-the-identity approximation;[27−29] see Figure 1. The def2-TZVP basis set was used along with an implicit solvent model for water.[30] These calculations indicate that the absorption corresponds to an $S_1 \leftarrow S_0$ transition with $\pi-\pi^*$ character in line with previous work.[25,26,31,32] On closer inspection of the orbital character (inset Figure 1), there is the presence of charge transfer from the methoxy substituent ($-OCH_3$). We evaluated the effect of the methoxy substituent by performing the same RI-CC2 calculations on shinorine and porphyra-334 without the methoxy group. The predicted S_1 excitation energies for these structures were spectrally blue-shifted 12 nm, highlighting that the presence of the methoxy substituent reduces the highest occupied molecular orbital (HOMO) to lowest unoccupied molecular orbital (LUMO) band gap (section S2), in accord with experiments.[33]

The transient absorption spectra (TAS) of shinorine and porphyra-334 following photoexcitation at their respective λ_{max} are displayed as false color heat maps in Figure 2a,b and as lineouts in Figure 2c,d. Given that shinorine and porphyra-334 differ only by a single methyl group that is not directly part of the chromophore, it is unsurprising that both TAS are almost identical; we therefore elect to discuss the TAS together.

Three main features characterize the TAS of shinorine and porphyra-334. First, there is a ground state bleach (GSB) present from time zero (Δt = 0, where our photoexcitation, or "pump", and detection, or "probe" beams are temporally overlapped) around 340−350 nm, which is to be expected as the absorption profiles of shinorine and porphyra-334 extend to ∼350 nm (Figure 1). Additionally, at early Δt, stimulated emission is observed spanning ∼375−740 nm, which spectrally red-shifts over time. This feature, in part, concurs with reported fluorescence profiles, which supports our assignment.[11−13] The third feature is an excited state absorption (ESA) which grows in around 350−400 nm, suggestive of consecutive kinetics.

To extract excited state lifetimes associated with the experimentally observed photodynamics, a global sequential model was employed using the software package Glotaran.[34,35] For both MAAs, three lifetimes were required for the fit, shown in Table 1. Figure 2e,f displays transients at selected wavelengths

https://doi.org/10.1021/acs.jpclett.1c00728
J. Phys. Chem. Lett. 2021, 12, 3641−3646

Table 1. Lifetimes and Associated Errors Extracted from the Global Sequential Fit of Shinorine and Porphyra-334 Photoexcited at Their Respective λ_{max}

MAA	τ_1 (fs)	τ_2 (ps)	τ_3 (ps)
shinorine	190 ± 90	1.17 ± 0.09	>1900
porphyra-334	310 ± 90	1.11 ± 0.09	>1900

with the global fit (solid line) overlaying the data (open circles). The quality of the fit can be assessed through the associated residuals (Figure S12).

The first lifetime, τ_1, is on the order of a few hundred femtoseconds, which we assign to MAAs undergoing fast geometry relaxation along the S_1 reaction coordinate toward the S_1/S_0 conical intersection (CI). τ_1 for shinorine and porphyra-334 is in excellent accord with the previously predicted S_1 lifetimes for the model MAA chromophore investigated using nonadiabatic molecular dynamics.[36]

The second lifetime, τ_2, which is approximately 1.1 ps, is assigned to population traversing through the S_1/S_0 CI and subsequent vibrational cooling along the S_0 coordinate via vibrational energy transfer, both intramolecular and intermolecular (to the solvent). This results in the decay of two features: first, the stimulated emission at long probe wavelengths (evidenced by the mild stimulated emission out to 2 ps; see lineouts in Figure 2c,d and evolution associated difference spectra in Figure S12, both centered around 450−740 nm) and second, the decay of the vibrationally hot ground electronic state centered at ∼375 nm. The observed vibrational cooling is relatively fast, which we suggest is attributed to the large hydrogen bonding network that plays an important role in the vibrational relaxation of MAAs. This conclusion is based on both our earlier work, which demonstrated increased solvent polarity resulted in faster vibrational cooling for an MAA motif[14] and a previous computational study, which examined porphyra-334's efficient dissipation of absorbed energy in water.[32] Specifically, the charged nature of zwitterions strengthens the interaction between the solute and first hydration shell allowing for fast and efficient dissipation of excess energy to the extended hydrogen bonding network.[32] Furthermore, our assignment is supported by other ultrafast spectroscopic studies on similar molecules that have reported fast vibrational relaxation in the ground electronic state.[37−39]

The overall relaxation mechanism proposed *supra* is displayed as a schematic in Figure 3. To probe the apparent barrierless decay observed experimentally, we employed gas-phase excited state relaxations from the Franck−Condon geometry using time-dependent density functional theory. These calculations yielded a structure with negative excitation energy, suggesting the presence of a CI[40] and corroborating our experimental findings (sections S1.5 and S2 in the Supporting Information).

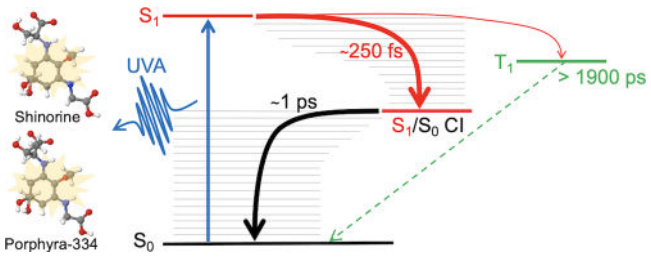

Figure 3. Schematic of the photoprotection mechanism of MAAs.

Indeed, this is in accord with previous calculations using CASSCF/CASPT2 methodology which predict a barrierless decay toward a CI dominated by an out-of-plane displacement of the ring substituents of MAAs.[31,36,41]

The final lifetime, τ_3 > 1900 ps, for both shinorine and porphyra-334, is attributed to any remaining species trapped in their excited state. The excited state refers to the S_1 state or the triplet state. Alternatively, this could be attributed to a photoproduct. As the fluorescence lifetime is ∼0.4 ns,[11−13] the latter two (triplet state or photoproduct) seem most likely. We add that our TEAS measurements were unable to detect any further stimulated emission out to 0.4 ns, a consequence of the very low fluorescence quantum yields (∼10^{-4}),[11−13] which would make observing this unlikely within our experimental signal-to-noise. For clarity, the inset of Figure 2c,d shows TAS at a Δt of 1900 ps. These spectra show the persistence of a GSB feature at ∼340 nm and two ESAs at ∼400 nm and ∼500−740 nm. Power dependency studies of the ESAs displayed single-photon induced dynamics for the former, assigned to triplet state formation (see later discussion) and two-photon induced dynamics for the latter, tentatively assigned to a solvated electron from the solvent (and/or solute, Figure S15), in accord with previous studies.[42,43] The former feature contributes toward the persistent GSB in the TEAS experiment. We add that two-photon induced dynamics are unlikely to be initiated by the sun or in our steady-state irradiations discussed *infra*.

The presence of a persistent GSB at extended time delays (Δt > 1900 ps), albeit very low in intensity, warrants further discussion. The GSB in the TAS of Figure 2 has (mostly) been omitted due to imperfect pump subtraction. At the expense of time resolution and signal intensity, a modification to our setup enabled imperfect pump subtraction to be greatly reduced allowing the GSB to be observed (sections S1.3 and S3.4). By assessing the signal intensity of the GSB at 0.1 and 1900 ps, we estimate that there is ≥95% GSB recovery within 1900 ps; the caveat here is we assume that there is no overlapping ESA (Figure S24). This indicates that nonradiative decay is the dominant relaxation mechanism for excited shinorine and porphyra-334, in accord with previous photoacoustic calorimetry findings.[12] Additional experiments following photoexcitation at 310 nm lend further support to this conclusion (section S3.4.2).

To further explore the resulting GSB, steady-state irradiation studies (see Figure 4) were performed to assess any photoproduct absorption. We observed very little degradation over a 5 h period in our samples (∼1%), in line with the previously reported photodegradation quantum yields and almost complete GSB recovery we observed in this study.[11−13] We add that liquid chromatography mass spectrometry after irradiation (not

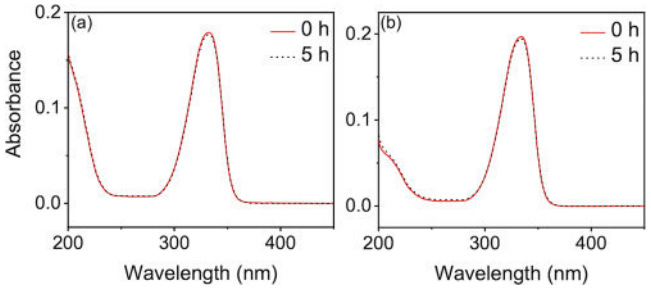

Figure 4. UV−visible spectra before and after 5 h of irradiation for (a) shinorine and (b) porphyra-334.

https://doi.org/10.1021/acs.jpclett.1c00728
J. Phys. Chem. Lett. 2021, 12, 3641−3646

shown) indicated the absence of new species absorbing at ~330 nm.

Comparison of the difference spectra between pre- and post-irradiated samples (Figure S25) and the 1900 ps TAS (Figure 2) for both MAAs shows that the two spectra do not correlate. While it is possible that some of the (very minor) incomplete GSB recovery is due to photoproduct formation, the absorption at 1900 ps (~350−450 nm) more closely resembles the previously reported triplet absorption.[11−13] As a result, we are confident that triplet state formation is the main source of incomplete GSB recovery.

Our triplet state predictions for the Franck−Condon geometry using RI-CC2 methodology found that the lower-lying T_1 (402 nm for shinorine and 403 nm for porphyra-334) is closest to the S_1;[27−29,44,45] see section S2 in the Supporting Information. Given that the orbital character of the S_1 and T_1 is the same, this plausibly explains the low quantum yield for intersystem crossing,[11,12] owing to El-Sayed's rule.[46] Further to this, as the triplet lifetime is on the microsecond time scale,[11,12] we propose that the triplet state mostly returns to the original ground state, accounting for the low amount of photodegradation observed in our irradiation studies.

We close the discussion by adding that the above experiments were also conducted on Helioguard 365 with little observed differences compared to the isolated MAA samples described within (section S5). This suggests that the efficacy of photoprotection is maintained in a more complex environment.

In summary, we have explored the blueprints of microbial photoprotection. By using TEAS for the first time to track the nonradiative energy flow in two MAAs shinorine and porphyra-334, we have linked their ultrafast relaxation dynamics with their unrivalled long-term photostability. Relaxation to the ground state and the consequent vibrational cooling occur within ~2 ps with at most 5% GSB not recovering within 1900 ps. If MAAs were present during the Archean Earth and experienced selection pressures, the consequent excited state dynamics reflects their unprecedented UV-screening properties. In highlighting nature's approach to photoprotection, this work can contribute to developments in a myriad of industries where molecular photon-to-heat converters have important applications.

■ ASSOCIATED CONTENT

Supporting Information

The Supporting Information is available free of charge at https://pubs.acs.org/doi/10.1021/acs.jpclett.1c00728.

Experimental details and sample characterization, computational methods and results, supporting results for shinorine and porphyra-334, and supporting results for Helioguard 365 sample (PDF)

■ AUTHOR INFORMATION

Corresponding Author

Vasilios G. Stavros − *Department of Chemistry, University of Warwick, Coventry CV4 7AL, United Kingdom;* orcid.org/0000-0002-6828-958X; Email: v.stavros@warwick.ac.uk

Authors

Abigail L. Whittock − *Department of Chemistry and Analytical Science Centre for Doctoral Training, Senate House, University of Warwick, Coventry CV4 7AL, United Kingdom;* orcid.org/0000-0001-6361-3291

Nazia Auckloo − *Department of Chemistry and Warwick Integrative Synthetic Biology Centre and School of Life Sciences, University of Warwick, Coventry CV4 7AL, United Kingdom*

Adam M. Cowden − *Department of Chemistry and Molecular Analytical Science Centre for Doctoral Training, Senate House, University of Warwick, Coventry CV4 7AL, United Kingdom*

Matthew A. P. Turner − *Department of Chemistry, University of Warwick, Coventry CV4 7AL, United Kingdom;* orcid.org/0000-0003-4213-1036

Jack M. Woolley − *Department of Chemistry, University of Warwick, Coventry CV4 7AL, United Kingdom*

Martin Wills − *Department of Chemistry, University of Warwick, Coventry CV4 7AL, United Kingdom;* orcid.org/0000-0002-1646-2379

Christophe Corre − *Department of Chemistry and Warwick Integrative Synthetic Biology Centre and School of Life Sciences, University of Warwick, Coventry CV4 7AL, United Kingdom*

Complete contact information is available at: https://pubs.acs.org/10.1021/acs.jpclett.1c00728

Notes

The authors declare no competing financial interest.

The underlying data for this publication can be found in the Zenodo data repository at DOI: 10.5281/zenodo.4428814.

■ ACKNOWLEDGMENTS

The authors would like to thank Mibelle Biochemistry for supplying the Helioguard 365 samples used within this letter, and the Warwick Centre for Ultrafast Spectroscopy (WCUS) for the use of the ultrafast spectroscopy equipment. Computing facilities were provided by the Scientific Computing Research Technology Platform of the University of Warwick. We acknowledge the use of Athena at HPC Midlands+, which was funded by the EPSRC by Grant No. EP/P020232/1, in this research, as part of the HPC Midlands+ consortium. A.L.W. thanks the University of Warwick and Lubrizol for funding a Ph.D. studentship through the Centre for Doctoral Training in Analytical Science. N.A. thanks the University of Warwick for a Ph.D. studentship though the Chancellor Scholarship. A.M.C. thanks the EPSRC for a Ph.D. studentship through the EPSRC Centre for Doctoral Training in Molecular Analytical Science, Grant No. EP/L015307/1. M.A.P.T. thanks the University of Warwick for funding. J.M.W. acknowledges the support of FetOpen grant BoostCrop (Grant Agreement 828753). This work was also supported by Grant BB/M017982/1 from the UK Biotechnology and Biological Sciences Research Council (BBSRC) and Grant EP/S021442/1 from the EPSRC. V.G.S. thanks the Royal Society and Leverhulme Trust for a Royal Society Leverhulme Trust Senior Research Fellowship, the Royal Society for a Royal Society Industry Fellowship, and the EPSRC (UK) under Grant No. EP/N010825/1. The authors thank Martin Lea for the help and useful discussion.

■ REFERENCES

(1) Cockell, C. S.; Knowland, J. Ultraviolet radiation screening compounds. *Biol. Rev. Cambridge Philos. Soc.* **1999**, *74*, 311−345.

(2) Rosic, N. N. Phylogenetic analysis of genes involved in mycosporine-like amino acid biosynthesis in symbiotic dinoflagellates. *Appl. Microbiol. Biotechnol.* **2012**, *94*, 29−37.

(3) Sinha, R. P.; Singh, S. P.; Häder, D. P. Database on mycosporines and mycosporine-like amino acids (MAAs) in fungi, cyanobacteria,

macroalgae, phytoplankton and animals. *J. Photochem. Photobiol., B* **2007**, *89*, 29−35.
(4) Oren, A.; Gunde-Cimerman, N. Mycosporines and mycosporine-like amino acids: UV protectants or multipurpose secondary metabolites? *FEMS Microbiol. Lett.* **2007**, *269*, 1−10.
(5) Bandaranayake, W. M. Mycosporines: are they nature's sunscreens? *Nat. Prod. Rep.* **1998**, *15*, 159−172.
(6) Shick, J. M.; Dunlap, W. C. Mycosporine-like amino acids and related Gadusols: biosynthesis, accumulation, and UV-protective functions in aquatic organisms. *Annu. Rev. Physiol.* **2002**, *64*, 223−262.
(7) Losantos, R.; Sampedro, D.; Churio, M. S. Photochemistry and photophysics of mycosporine-like amino acids and gadusols, nature's ultraviolet screens. *Pure Appl. Chem.* **2015**, *87*, 979−996.
(8) Woolley, J. M.; Stavros, V. G. Unravelling photoprotection in microbial natural products. *Sci. Prog.* **2019**, *102*, 287−303.
(9) Abiola, T. T.; Whittock, A. L.; Stavros, V. G. Unravelling the Photoprotective Mechanisms of Nature-Inspired Ultraviolet Filters Using Ultrafast Spectroscopy. *Molecules* **2020**, *25*, 3945.
(10) Lucas, R.; McMicheal, T.; Smith, W.; Armstrong, B., Solar ultraviolet radiation. Global burden of disease from solar ultraviolet radiation. In *Environmental Burden of Disease Series, No. 13*; World Health Organization: Geneva, Switzerland, 2006.
(11) Conde, F. R.; Churio, M. S.; Previtali, C. M. The photoprotector mechanism of mycosporine-like amino acids. Excited-state properties and photostability of porphyra-334 in aqueous solution. *J. Photochem. Photobiol., B* **2000**, *56*, 139−144.
(12) Conde, F. R.; Churio, M. S.; Previtali, C. M. The deactivation pathways of the excited-states of the mycosporine-like amino acids shinorine and porphyra-334 in aqueous solution. *Photochem. Photobiol. Sci.* **2004**, *3*, 960−967.
(13) Orallo, D. E.; Bertolotti, S. G.; Churio, M. S. Photophysicochemical characterization of mycosporine-like amino acids in micellar solutions. *Photochem. Photobiol. Sci.* **2017**, *16*, 1117−1125.
(14) Woolley, J. M.; Staniforth, M.; Horbury, M. D.; Richings, G. W.; Wills, M.; Stavros, V. G. Unravelling the Photoprotection Properties of Mycosporine Amino Acid Motifs. *J. Phys. Chem. Lett.* **2018**, *9*, 3043−3048.
(15) Losantos, R.; Lamas, I.; Montero, R.; Longarte, A.; Sampedro, D. Photophysical characterization of new and efficient synthetic sunscreens. *Phys. Chem. Chem. Phys.* **2019**, *21*, 11376−11384.
(16) Whittock, A. L.; Turner, M. A. P.; Coxon, D. J. L.; Woolley, J. M.; Horbury, M. D.; Stavros, V. G. Reinvestigating the Photoprotection Properties of a Mycosporine Amino Acid Motif. *Front. Chem.* **2020**, *8*, 574038.
(17) Woolley, J. M.; Losantos, R.; Sampedro, D.; Stavros, V. G. Computational and experimental characterization of novel ultraviolet filters. *Phys. Chem. Chem. Phys.* **2020**, *22*, 25390−25395.
(18) Takano, S.; Nakanishi, A.; Uemura, D.; Hirata, Y. Isolation and structure of a 334 nm UV-absorbing substance, porphyra-334 from the red alga *Porphyra tenera* Kjellman. *Chem. Lett.* **1979**, *8*, 419−420.
(19) Tsujino, I.; Yabe, K.; Sekikawa, I. Isolation and structure of a new amino acid, shinorine, from the red alga, *Chondrus yendoi* Yamada et Mikami. *Bot. Mar.* **1980**, *23*, 65−68.
(20) Schmid, D.; Schürch, C.; Zülli, F.; Nissen, H.-P.; Prieur, H. Mycosporine-like amino acids: Natural UV-screening compounds from red algae to protect the skin against photoaging. *SÖFW J.* **2003**, *129*, 1−5.
(21) Schmid, D.; Schürch, C.; Zülli, F. UVA-screening compounds from red algae protect against photoageing. *Pers. Care* **2004**, 29−31.
(22) Schmid, D.; Schürch, C.; Zülli, F. UV-A sunscreen from red algae for protection against premature skin aging. *Cosmet. Toilet. Manuf. Worldw.* **2004**, 139−143.
(23) Schmid, D.; Schürch, C.; Zülli, F. Mycosporine-like Amino Acids from Red Algae Protect against Premature Skin-Aging. *Euro Cosmet.* **2006**, 1−4.
(24) *TURBOMOLE* V7.4 2019, a development of University of Karlsruhe and Forschungszentrum Karlsruhe GmbH, 1989−2007, TURBOMOLE GmbH, since 2007; available from http://www.turbomole.com.
(25) Matsuyama, K.; Matsumoto, J.; Yamamoto, S.; Nagasaki, K.; Inoue, Y.; Nishijima, M.; Mori, T. pH-Independent Charge Resonance Mechanism for UV Protective Functions of Shinorine and Related Mycosporine-like Amino Acids. *J. Phys. Chem. A* **2015**, *119*, 12722−12729.
(26) Hatakeyama, M.; Koizumi, K.; Boero, M.; Nobusada, K.; Hori, H.; Misonou, T.; Kobayashi, T.; Nakamura, S. Unique Structural Relaxations and Molecular Conformations of Porphyra-334 at the Excited State. *J. Phys. Chem. B* **2019**, *123*, 7649−7656.
(27) Christiansen, O.; Koch, H.; Jørgensen, P. The second-order approximate coupled cluster singles and doubles model CC2. *Chem. Phys. Lett.* **1995**, *243*, 409−418.
(28) Hättig, C.; Weigend, F. CC2 excitation energy calculations on large molecules using the resolution of the identity approximation. *J. Chem. Phys.* **2000**, *113*, 5154−5161.
(29) Hättig, C.; Köhn, A. Transition moments and excited-state first-order properties in the coupled-cluster model CC2 using the resolution-of-the-identity approximation. *J. Chem. Phys.* **2002**, *117*, 6939−6951.
(30) Weigend, F.; Häser, M.; Patzelt, H.; Ahlrichs, R. RI-MP2: optimized auxiliary basis sets and demonstration of efficiency. *Chem. Phys. Lett.* **1998**, *294*, 143−152.
(31) Sampedro, D. Computational exploration of natural sunscreens. *Phys. Chem. Chem. Phys.* **2011**, *13*, 5584−5586.
(32) Koizumi, K.; Hatakeyama, M.; Boero, M.; Nobusada, K.; Hori, H.; Misonou, T.; Nakamura, S. How seaweeds release the excess energy from sunlight to surrounding sea water. *Phys. Chem. Chem. Phys.* **2017**, *19*, 15745−15753.
(33) Dunlap, W. C.; Chalker, B. E.; Bandaranayake, W. M.; Wu Won, J. J. Nature's sunscreen from the Great Barrier Reef, Australia. *Int. J. Cosmet. Sci.* **1998**, *20*, 41−51.
(34) Mullen, K. M.; van Stokkum, I. H. M. TIMP: An R Package for Modeling Multi-way Spectroscopic Measurements. *J. Stat. Softw.* **2007**, *18*, 1−46.
(35) Snellenburg, J. J.; Laptenok, S.; Seger, R.; Mullen, K. M.; van Stokkum, I. H. M. Glotaran: A Java-Based Graphical User Interface for the R Package TIMP. *J. Stat. Softw.* **2012**, *49*, 1−22.
(36) Losantos, R.; Funes-Ardoiz, I.; Aguilera, J.; Herrera-Ceballos, E.; García-Iriepa, C.; Campos, P. J.; Sampedro, D. Rational Design and Synthesis of Efficient Sunscreens To Boost the Solar Protection Factor. *Angew. Chem., Int. Ed.* **2017**, *56*, 2632−2635.
(37) Pecourt, J.-M. L.; Peon, J.; Kohler, B. DNA Excited-State Dynamics: Ultrafast Internal Conversion and Vibrational Cooling in a Series of Nucleosides. *J. Am. Chem. Soc.* **2001**, *123*, 10370−10378.
(38) Shigeto, S.; Dlott, D. D. Vibrational relaxation of an amino acid in aqueous solution. *Chem. Phys. Lett.* **2007**, *447*, 134−139.
(39) Grieco, C.; Kohl, F. R.; Hanes, A. T.; Kohler, B. Probing the heterogeneous structure of eumelanin using ultrafast vibrational fingerprinting. *Nat. Commun.* **2020**, *11*, 4569.
(40) Toniolo, A.; Ben-Nun, M.; Martínez, T. J. Optimization of Conical Intersections with Floating Occupation Semiempirical Configuration Interaction Wave Functions. *J. Phys. Chem. A* **2002**, *106*, 4679−4689.
(41) Losantos, R.; Churio, M. S.; Sampedro, D. Computational Exploration of the Photoprotective Potential of Gadusol. *ChemistryOpen* **2015**, *4*, 155−160.
(42) Arai, S.; Sauer, M. C., Jr. Absorption Spectra of the Solvated Electron in Polar Liquids: Dependence on Temperature and Composition of Mixtures. *J. Chem. Phys.* **1966**, *44*, 2297−2305.
(43) Peon, J.; Hess, G. C.; Pecourt, J.-M. L.; Yuzawa, T.; Kohler, B. Ultrafast Photoionization Dynamics of Indole in Water. *J. Phys. Chem. A* **1999**, *103*, 2460−2466.
(44) Hättig, C.; Hald, K. Implementation of RI-CC2 triplet excitation energies with an application to trans-azobenzene. *Phys. Chem. Chem. Phys.* **2002**, *4*, 2111−2118.
(45) Hättig, C.; Köhn, A.; Hald, K. First-order properties for triplet excited states in the approximated coupled cluster model CC2 using an explicitly spin coupled basis. *J. Chem. Phys.* **2002**, *116*, 5401−5410.

https://doi.org/10.1021/acs.jpclett.1c00728
J. Phys. Chem. Lett. 2021, 12, 3641−3646

(46) El-Sayed, M. A. Spin—Orbit Coupling and the Radiationless Processes in Nitrogen Heterocyclics. *J. Chem. Phys.* **1963**, *38*, 2834–2838.

https://doi.org/10.1021/acs.jpclett.1c00728
J. Phys. Chem. Lett. 2021, 12, 3641−3646